American Journal of Pathology, Vol. 164, No. 1, January 2004

Early Adaptive Responses of the Vascular Wall during Venous Arterialization in Mice

Stephanie Kwei,* George Stavrakis,† Masaya Takahas,‡ George Taylor,§¶ M. Judah Folkman,*¶ Michael A. Gimbrone, Jr.,†¶ and Guillermo García-Cardeña†¶

From the Surgical Research Laboratories, Children's Hospital, Boston; the Department of Pathology,† Brigham and Women's Hospital, Boston; the Department of Radiology,‡ Beth Israel Deaconess Medical Center, Boston; the Department of Radiology,§ Children's Hospital, Boston; and Harvard Medical School,¶ Boston, Massachusetts*

Venous arterialization occurs when a vein segment is transposed as a bypass graft into the arterial circulation, resulting in a structural and functional reorganization of the vascular wall in response to the new local biomechanical environment. Although the anatomical changes of venous arterialization have been well characterized, the molecular mechanisms of vascular remodeling remain incompletely understood. Here, we present a novel model of venous arterialization in mice wherein the external jugular vein is connected to the common carotid artery. The hemodynamic characteristics of the arterialized vein, as assessed by ultrasound and magnetic resonance imaging, resemble features of the arterial circulation. Temporal analyses of the morphological changes in the venous segment at 1, 3, and 7 days after surgery demonstrate preservation of the endothelium at all time points and formation of multiple smooth muscle layers by day 7. Expression of endothelial E-selectin and VCAM-1 was documented at early time points, concomitant with the presence of neutrophils and monocytes/macrophages in the vascular wall. In addition, endothelium-dependent permeability was decreased in the arterialized vein when compared to the contralateral control vein. Thus, this novel mouse model of venous arterialization displays anatomical and cellular features present in other species, and should help to characterize the molecular mechanisms of this adaptive response of the vascular wall to changes in its biomechanical environment. ***(Am J Pathol 2004, 164:81–89)***

The interposition of a venous segment into the arterial circulation, as occurs during coronary artery bypass surgery, results in an adaptation of the vascular wall to the new biomechanical conditions.[1] The shift of the local environment engenders reorganization of the venous vascular architecture, such that over time, the venous graft acquires an artery-like structure. This vascular remodeling involves alterations in cell proliferation, cell death, cell migration, and degradation and/or production of extracellular matrix components.[2] Although the rearrangement of cellular and extracellular components is well described, little is known about how these events are physiologically and temporally coordinated due to the complexity of the integrated response elicited by arterial biomechanical cues. While many *ex vivo* and *in vivo* models have been designed to resemble the adaptive responses of venous bypass grafts, relatively few approaches have been developed in the murine system to take advantage of the genetic and genomic tools available in that species. As a result, although interactions among vascular cells, their substrates, and the local environment are known to contribute to vascular remodeling, our understanding of the basic biology of venous arterialization remains incomplete.

Exposure to the new biomechanical environment of the arterial circulation is thought to be an important stimulus for the vascular remodeling of a venous bypass graft.[3] Several anatomical and cellular changes in grafted veins have been documented. For example, in a model of canine femoral vein grafts, arterialized veins appear thicker than normal saphenous veins, with infiltration of polymorphonuclear leukocytes into the medial layer 2 days after surgery.[4] Moreover, a role for the extracellular matrix and its regulators (matrix metalloproteinases, MMPs) has been established. Thus, when human saphenous vein segments were perfused *ex vivo* under arterial *versus* venous conditions, a significant increase in the production of MMP-9 and MMP-2 under arterial flow was observed, together with increased secretion of MMP-9 and higher retention of MMP-2 in the extracellular space.[5,6] In humans, tenascin-C expression has been documented in the media and adventitia of patent saphe-

Supported by grants from National Heart, Lung and Blood Institute (NHLBI), National Institutes of Health (NIH) (P50-HL56985 to M.A.G.), NIH (R01 CA64481–08 to J.F.), The Society of University Surgeons (to S.K.), The Abbott Trust at Children's Hospital (to J.F. and G.G.-C.), and The Leet Patterson Trust (to G.G.-C. and S.K.).

Accepted for publication September 17, 2003.

Address reprint requests to Guillermo García-Cardeña, Ph.D, Department of Pathology, Harvard Medical School, Center for Excellence in Vascular Biology, Brigham and Women's Hospital, 77 Avenue Louis Pasteur, HMS/NRB-730C, Boston, MA 02115. E-mail: ggarcia-cardena@rics.bwh.harvard.edu.

nous vein grafts but not in occluded grafts or normal arteries and veins.[7]

Furthermore, several large animal models of vein bypass grafts were developed to characterize in detail venous arterialization *in vivo*.[8,9,10,11] In a well-characterized rabbit model of jugular vein interposition into the carotid artery, arterialized veins demonstrated altered sensitivity to bradykinin,[12] norepinephrine, histamine, serotonin,[13] adenosine,[14] and dopamine.[15] Tissue factor expression was increased in the vessel intima 3 days after grafting, but was not detected 14 or 28 days after grafting.[16] There was also differential expression of collagen III and IV over time in the arterialized bypass grafts.[17] In addition, changes in gene expression have been characterized, such as down-regulation of endothelin B receptors[18] and an initial reduction in thrombomodulin expression by the luminal endothelium.[19] Vascular endothelial growth factor mRNA expression was increased in vein grafts of dogs[20] and rats.[21]

While arterialization of venous bypass grafts involves numerous remodeling processes, the initial adaptation of the vein segment may subsequently lead to significant vascular pathologies. Several animal models have been designed to resemble the pathological consequences of venous arterialization. For example, in mice, arteriosclerotic and neointimal hyperplastic lesions were induced in arterialized veins using vascular cuffs or an end-to-side surgical anastomosis.[22,23] Using the model originally described by Zou et al,[22] the role of specific genes in the development of accelerated atherosclerotic lesions was assessed.[24,25,26] Although these murine models allow for the study of venous graft pathology, the normal early physiological adaptive response of the venous vessel to the arterial circulation remains elusive. Here, we developed a novel model of venous arterialization in mice by creating an arterio-venous connection between the common carotid artery and the external jugular vein *in situ*, and described the early morphological and functional changes of a vein exposed to the arterial circulation.

Materials and Methods

Surgical Procedure

C57BL/6J male mice, 8 to 10 weeks old, were anesthetized by intraperitoneal injection of Avertin (tribromoethanol, Fisher Scientific, Pittsburgh, PA) 125 to 240 mg/kg. Analgesia was administered pre-operatively as a subcutaneous injection of Buprenex (buprenorphine) 0.05 to 0.1 mg/kg. After adequate shaving and preparation of the neck skin, a 1-cm right paramidline vertical incision was made through skin and fascia. The cervical fat was dissected and excised to expose the external jugular vein (JV). All branches of the JV were ligated using 10–0 ethilon (Ethicon, Somerville, NJ) and divided. The JV was clamped distally and ligated proximally with 8–0 silk (Ethicon) and divided. The common carotid artery (CCA) was clamped proximally and ligated just below the carotid bifurcation with 8–0 silk. A perfluorocarbon biocompatible microvascular catheter (Fine Science Tools, San Francisco, CA), measuring 400 μm in outer diameter and 200 μm in inner diameter, was cut into 2-mm segments and soaked in heparin (100 units/ml) before the surgical intervention. A carotid arteriotomy was made between the proximal clamp and distal ligation, and the catheter was inserted into the CCA proximally and the JV distally. The catheter was secured to both vessels by circumferential ligation using 8–0 silk. The CCA was divided between the distal ligation and catheter. Upon removal of the microvascular clamps, pulsatile flow was visualized in the JV. Sham surgery was performed in which cervical dissection was completed, and all branches of the JV were ligated and divided using 10–0 ethilon. A microvascular catheter was placed adjacent to the JV. In all cases, the skin was closed using 4–0 vicryl in a continuous fashion. Operative time averaged 40 to 60 minutes. All animal procedures were performed with approval from the Institutional Animal Care and Use Committee.

Imaging and Hemodynamic Analysis

Magnetic resonance angiography (MRA) was performed with an 8.5 Tesla micro imaging system, operating at 360 MHz proton frequency (DRX-360, Burker BioSpin MRI, Inc, Karlsruhe, Germany). Mice were anesthetized by inhalation of 1 to 2% isofluorane and placed in a radio frequency coil (I.D. 20 mm). After localizer images, a two-dimensional phase contrast (PC) sequence was conducted over the entire neck region. The imaging parameters were as follows: repetition time/echo time, 20 to 25 msec/5.5 msec; field of view, 16 $\times$ 16 mm^2; slice thickness, 1 mm; number of slices, 16 to 18; matrix size 128 $\times$ 128; number of excitations, 4; flip angle, 60 degrees; and the velocity-encoding coefficient, 10 cm/sec. The maximum intensity projection (MIP) as post-processing technique was applied to all PC MR images in each animal. The total imaging time was 9 to 11 minutes. Mice were imaged 1 day and 7 days after surgery.

Duplex Doppler ultrasound was performed on the right, surgical arterialized JV and the left, non-surgical CCA and JV. Mice were anesthetized by intraperitoneal injection of Avertin (tribromoethanol) 125 to 240 mg/kg. Imaging was performed using a high-resolution linear transducer operating at a scanning frequency of 15 MHz. The field of view was limited to the most superficial (5 mm) structures of the neck. Scale, wall filter, and gain settings were optimized for both color and pulsed Doppler studies. Each vessel was identified by color Doppler, and lumenal diameter of the vessel was obtained by placing measurement calipers on the frozen video display of a representative color image of each vessel. A sample volume measuring $<$2 mm was placed over each vessel for hemodynamic sampling during real-time scanning. Multiple sampling of flow was obtained for at least 5 consecutive seconds on each vessel of interest. Mice were imaged 1 day and 7 days after surgery.

Tissue Isolation

Vessels were harvested at 1 day, 3 days, and 7 days after surgery. At the time of harvest, the animals were anes-

thetized under inhaled isofluorane, and the arterialized vein was exposed through the previous incision. Graft patency was confirmed by the visual appearance of pulsatile arterial blood flow in the external jugular vein. After confirmation of patency, the abdominal and thoracic cavities were opened by a midline incision. The animal was euthanised under anesthesia by cardiac puncture and incision of the left renal vein. The animal was perfusion-fixed (110 mm Hg) using phosphate-buffered saline (PBS) followed by 2% paraformaldehyde through the left ventricle. A 4-mm segment of the arterialized vein was isolated distal to the microvascular catheter anastomosis, and the contralateral JV was harvested as a control at all times studied. All vessels were dissected from the surrounding tissue and fat. The vessels were immediately oriented and snap-frozen in OCT for further analysis.

Immunohistochemical Analysis

Sequential 5-μm sections of the arterialized vein, beginning 1 mm distal to the anastomosis of the microvascular catheter, and the contralateral JV control vessel were processed for histology and immunohistochemistry. Hematoxylin and eosin staining was performed for gross morphological examination. All sections were mounted using Permount (Fisher, Medford, MA).

Frozen sections were fixed with acetone, blocked with normal serum, avidin, and biotin solutions, and then incubated with primary antibody for 1 hour at room temperature under moist conditions. Sections were sequentially treated with goat anti-rat biotin at 1:200 dilution (Jackson Immunochemicals, West Grove, PA), blocked for endogenous peroxidase using 0.3% hydrogen peroxide for 20 minutes, and then treated with the ABC-Elite peroxidase kit (Vector Laboratory, Burlingame, CA). Finally, sections were developed using AEC chromagen and counterstained with Gill's hematoxylin No. 2. Negative controls were performed for all antibodies by substituting an isotype-match antibody.

Serial sections were stained with anti-α-smooth muscle actin (1:150) conjugated to alkaline phosphatase (Sigma, St. Louis, MO) and developed with Fast Red (Vector Laboratory) for 30 minutes at room temperature. Vessels were also labeled with a mouse monoclonal antibody against proliferating cell nuclear antigen (PCNA, BD Biosciences, San Diego, CA), following incubation with rat anti-mouse CD16/CD32 to block the mouse Fc receptors. Sections were also analyzed for the presence of vascular endothelium (CD31, BD Biosciences), E-selectin (BD Biosciences), vascular cell adhesion molecule (VCAM-1, BD Biosciences), neutrophils (Gr-1, BD Biosciences), and monocytes and macrophages (Mac-1/CD11b, Biodesign, Saco, ME). The terminal deoxynucleotidyl transferase-mediated dUTP-biotin nick end-labeling assay (TUNEL, Intergen Company, Purchase, NY) was performed for *in situ* detection of apoptotic bodies.

Permeability Assay

Under general anesthesia, mice from all time points were injected with Evans Blue dye (60 mg/kg) via the left retro-orbital plexus, 30 minutes before euthanasia, followed by harvest of the arterialized vein and the contralateral JV and CCA. All vessels were rinsed in PBS. Another group of 7-day post-surgery mice were given recombinant human vascular endothelial growth factor (rhVEGF, 300 ng) by right retro-orbital injection, 10 minutes after receiving Evans Blue dye, and 30 minutes before vessel harvest.

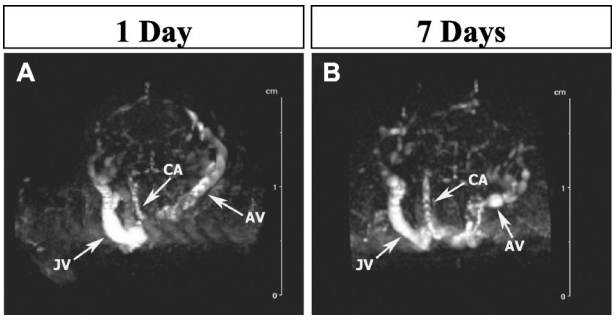

Figure 1. Magnetic resonance angiogram (MRA) of the surgical model represented as the cumulative reconstruction of 18 MRA images. Phase contrast imaging technique allows visualization of blood flow, and stationary tissues are not visualized. **A:** MRA of a mouse 1 day after surgery. The surgical CCA is oriented perpendicular to the image plane and is therefore not visible. **Bar**, 2 cm. **B:** MRA of a mouse 7 days after surgery provides non-invasive confirmation of vascular patency. JV and CCA, contralateral external jugular vein and common cartotid artery, respectively; AV, arterialized vein.

Statistics

Data are expressed as mean ± SD. Comparisons were made using a two-tailed Student's *t*-test. Differences were considered to be significant at $P < 0.01$.

Results

Creation of an Arterio-Venous Connection

We performed this surgery in a total of 17 mice, and at the time of vessel harvest, 11 vessels were found to be patent (65% overall success rate). Thus, a minimum of three mice was studied at each time point for changes in vessel morphology and immunohistochemical analyses. The major cause of failure was thrombosis, therefore, venous segments that appeared thrombosed were excluded from analysis. Vascular patency was confirmed before vessel perfusion and harvest by the gross appearance of pulsatile arterial blood flow in the external jugular vein.

Non-Invasive Imaging and Hemodynamic Characteristics

To assess vessel patency and the overall anatomical features of the surgical model we performed magnetic resonance angiography (MRA) in the head and neck region of mice 1 day and 7 days after surgery. Blood flow was visualized in the non-surgical JV and CCA, and the surgical JV exposed to the carotid arterial circulation (Figure 1). As is typical for MRA imaging, stationary tissues were not visualized secondary to post-processing

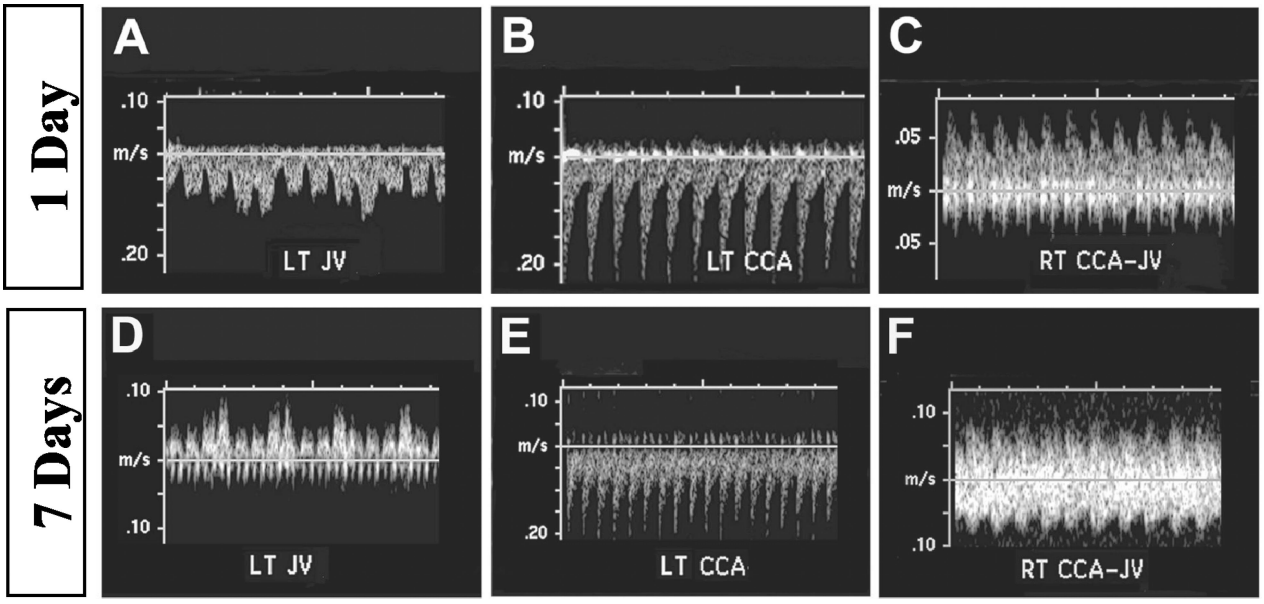

Figure 2. Duplex ultrasound of the arterialized vein 1 day and 7 days after surgery. **A** and **D:** Tracing from the contralateral control external jugular vein (LT JV) is characterized by a pattern of irregular pulsatility related to retrograde transmission of right atrial and ventricular pressure pulses, as well as respiratory variability. **B** and **E:** Tracing from the contralateral control common carotid artery (LT CCA) shows a brief and sharp systolic upstroke with relatively little forward flow at the end of diastole. **C** and **F:** Pulsed Doppler waveforms obtained from the arterialized venous segment (RT CCA-JV) show an unvarying pattern of pulsatile flow with prominent forward flow during diastole. Pulsatility was indistinguishable from the mouse's heart rate, suggesting transmitted arterial pulsations into the lower resistance venous segment.

suppression techniques. Interestingly, the JV exposed to arterial flow demonstrated an increased diameter distally in comparison to the distal contralateral JV.

To characterize the waveforms of the arterialized vein and contralateral control vessels, we performed duplex ultrasonography. At 1 day and 7 days after surgery, duplex ultrasound showed that the hemodynamic features of the right arterialized vein differ from the CCA and JV on the left, non-surgical side. Hemodynamics of the control JV (Figure 2,A and D) demonstrated a pattern of normal venous flow with respiratory variation and retrograde cardiac pulsations of variable amplitude. The JV exposed to arterial flow (Figure 2, C and F) showed little respiratory variation and a pattern of pulsatility that was directly related to the cardiac cycle; it was of continuous but lower amplitude compared to normal arterial pulsatility in the contralateral CCA (Figure 2, B and E). In addition, flow during diastole was higher than that observed in the contralateral CCA.

Remodeling of the Vascular Wall

To determine the early morphological changes in the venous vascular wall in response to the arterial circulation, an immunohistochemical study was performed at 1, 3, and 7 days after surgery. All sections were derived from the JV exposed to the arterial circulation 1 mm distal to the microvascular catheter anastomosis. As controls we used the contralateral JV for each time point. No differences were observed among time 0 controls and 1, 3, and 7 days post-surgery JV contralateral controls. Thus, all figures show one representative control. Hematoxylin and eosin-stained sections demonstrated alterations in the venous vascular wall at the earliest time point studied, 24 hours after surgery. On postoperative day 1, the presence of an acellular band surrounding the vessel lumen was noticed (Figure 3B) with a concomitant increase in the number of cells present in the vascular wall (Figure 3F) when compared to controls (Figure 3E). After 3 days, the acellular layer was replaced by cellular components, which appeared disorganized (Figure 3G) and non-uniform around the vessel lumen (Figure 3C). At 7 days, however, the cellular layers around the vascular wall appeared in organized layers (Figure 3, D and H). Circumferential media thickening was quantitatively assessed at this time point (control, 9.78 μm $\pm$ 0.77, $n = 3$; and 7-days post-surgery 44.40 μm $\pm$ 5.84*, $n = 3$; asterisk indicate that this value is significantly different from control value; $P < 0.01$). As arterialization of the external jugular vein progressed, the vessel also acquired a more elastic quality, as seen by the wide lumen of the arterialized vein after 7 days (Figure 3D) in comparison to the typical collapsed lumen of the control vein (Figure 3A).

To assess endothelial integrity in this surgical model, we examined serial sections from vessels at 1, 3, and 7 days after surgery. At all time points studied, there was no evidence of endothelial cell denudation or disruption of the monolayer (Figure 4). Furthermore, after 7 days there was evidence of neovascularization in the vascular wall by the appearance of microvessels (Figure 4D).

To confirm the identity of the cells abluminally adjacent to the endothelium, we stained vessel cross-sections for smooth muscle actin. Before arterialization, the external jugular vein had a single layer of smooth muscle actin expression in the vascular wall (Figure 5A). After 24 hours of arterial circulation, the subendothelial cell layer showed smooth muscle actin expression (Figure 5B). Three days after surgery, smooth muscle actin expres-

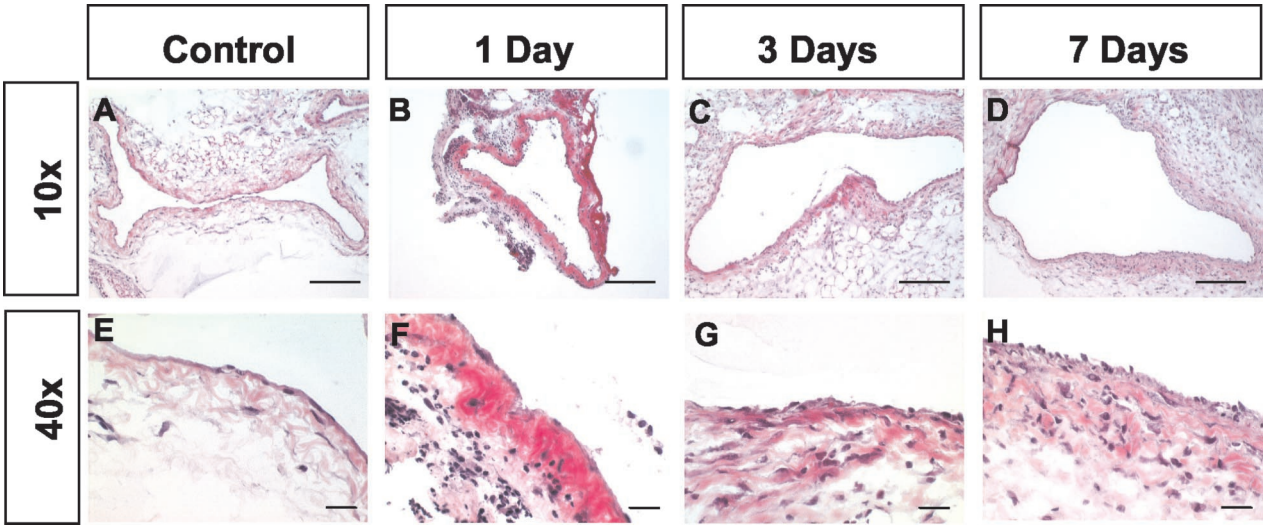

Figure 3. Morphological changes of the venous vascular wall in response to the arterial biomechanical environment visualized by hematoxylin and eosin staining. **A** and **E:** Contralateral control external jugular vein (JV) shows a single layer of endothelial cells lining the vascular lumen. **B** and **F:** The JV 24 hours after exposure to arterial flow. Note the uniform **band** of acellular connective tissue outlining the vascular lumen. There is also an increase of cells in the vascular wall. **C** and **G:** The acellular layer is replaced by a disorganized arrangement of cells 3 days after surgery. **D** and **H:** Several organized cellular layers appear in the vascular wall 7 days after surgery. **Bars**, 60 μm (**A–D**). **Bars**, 30 μm (**E–H**).

sion was found in several cells of the remodeling media (Figure 5C). After 7 days, smooth muscle actin expression appeared in well-organized concentric layers of the vascular wall (Figure 5D).

To determine the role of cellular proliferation in the adaptive changes of the vascular wall, vessels were stained with an antibody against proliferating cell nuclear antigen (PCNA). In the contralateral control vessels, there was no evidence of proliferating cells (Figure 5E), however, within 24 hours of arterialization, there were positively stained cells in the endothelial layer and other regions of the vascular wall (arrows, Figure 5F). After 3 days, proliferating cells were more prevalent in the vascular wall in comparison to the endothelium (arrow, Figure 5G), and by 7 days, the proliferative activity was infrequent in the vascular wall, consistent with the location of smooth muscle actin expression (Figure 5H). Thus, proliferation of smooth muscle cells may have contributed to the increase in vascular wall thickness and mass after 7 days of exposure to the arterial circulation.

To assess for the incidence of apoptosis during vascular remodeling in this model, we performed the terminal deoxynucleotidyl transferase-mediated dUTP-biotin nick end-labeling (TUNEL) assay. Using this analysis, we found little evidence of apoptosis. Only a few TUNEL-positive cells were located in the vascular wall at 1 day (Figure 5J), with the highest number of apoptotic cells observed at 3 days (Figure 5K). There was no apoptotic activity after 7 days of arterialization (Figure 5L), and

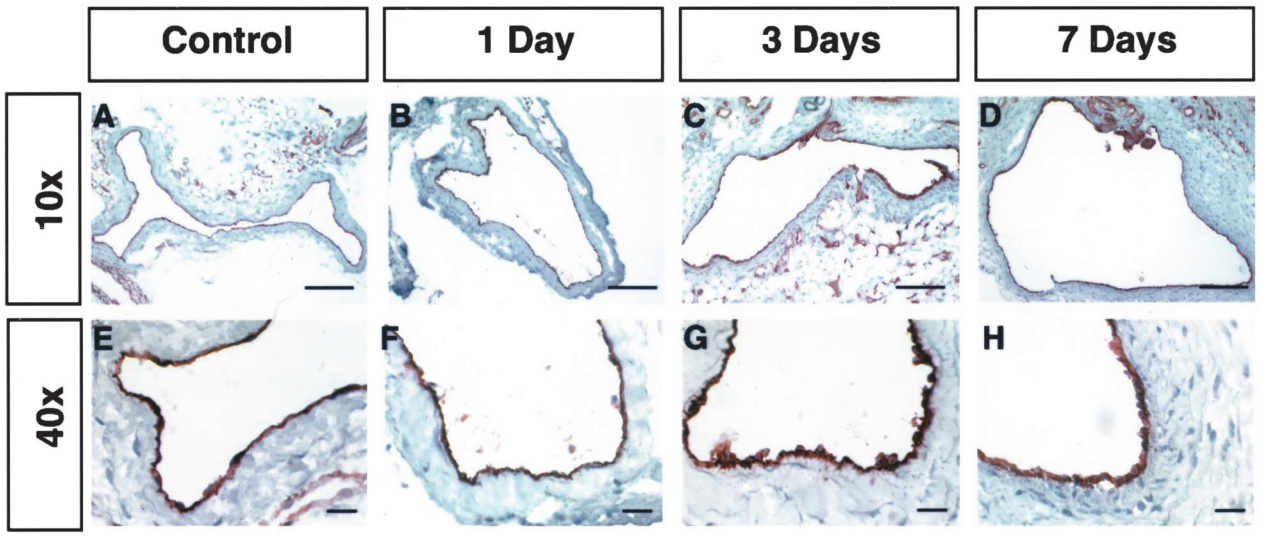

Figure 4. CD31 staining demonstrates the preservation of endothelial integrity during venous arterialization. **A** and **E:** CD31 expression in the contralateral control external jugular vein (JV). **B** and **F:** The JV 24 hours after exposure to the arterial circulation. **C** and **G:** The JV 3 days after surgery. **D** and **H:** After 7 days, the endothelial cell layer remains intact. Note the appearance of microvessels in the outer vascular wall. **Bars**, 160 μm (**A–D**). **Bars**, 30 μm (**E–H**).

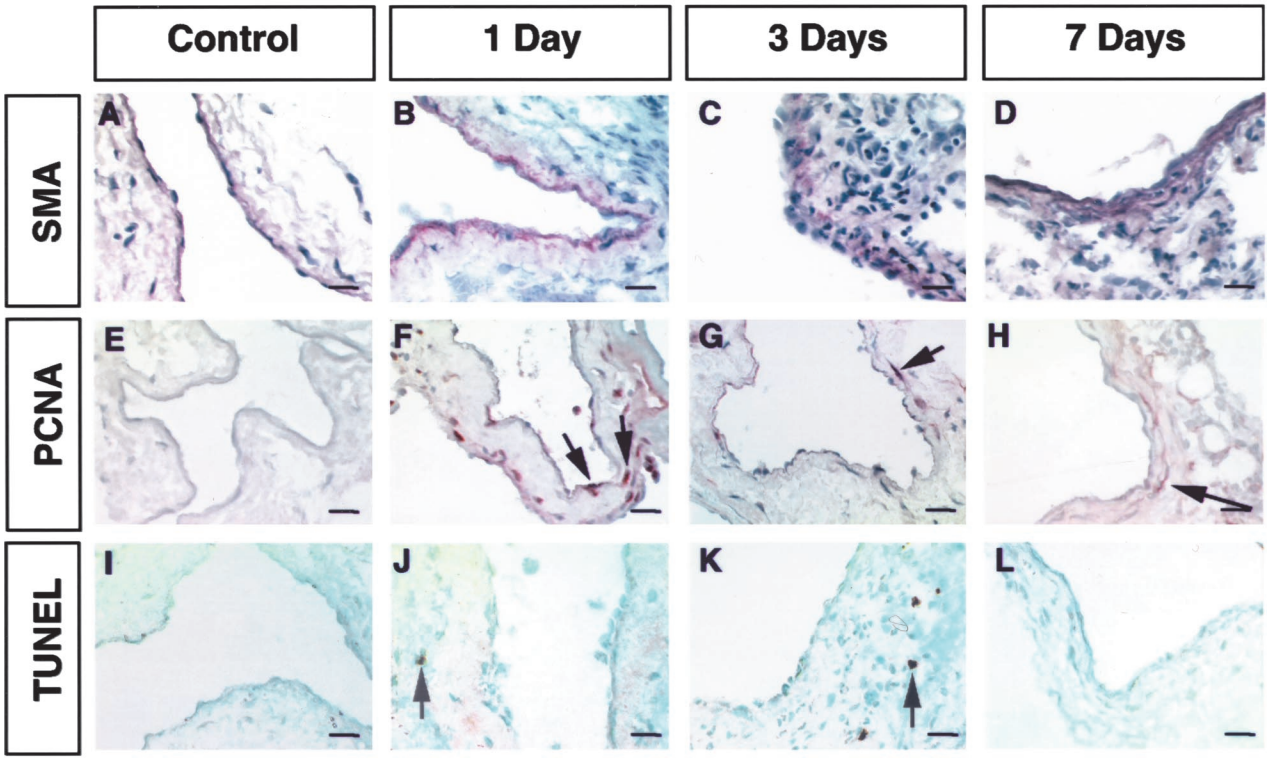

Figure 5. Expression of α-smooth muscle actin and markers of proliferation and apoptosis. **A:** The control external jugular vein (JV) shows a single subendothelial layer of smooth muscle actin expression. **B:** The JV 24 hours after exposure to the arterial circulation shows smooth muscle actin expression along the subendothelial layer of the vascular wall. **C:** After 3 days, smooth muscle actin expression is found in several cells below the endothelial layer. **D:** The vascular wall 7 days after surgery demonstrates organized concentric layers of cells expressing smooth muscle actin. **E:** The control JV shows no proliferative activity in the vascular wall. **F:** One day after surgery, cells in the endothelial layer (**arrow**) and other sites of the vascular wall (**arrow**) demonstrate proliferative activity. **G:** Proliferation is more apparent at 3 days in the vascular wall just below the endothelium (**arrow**). **H:** Proliferating cells correspond to areas of smooth muscle actin expression after 7 days of arterialization (**arrow**). **I:** The control JV demonstrates no apoptotic activity. **J:** One day after surgery, a small number of cells in the vascular wall shows signs of apoptosis. **K:** More apoptotic cells in the vascular wall are seen 3 days after surgery, but none localize to the endothelium or smooth muscle layers. **L:** After 7 days of arterialization, there is no evidence of apoptotic activity in the vascular wall. **Bars**, 30 μm.

control vessels demonstrated no evidence of apoptosis at all time points examined (Figure 5I).

Expression of Adhesion Molecules and Presence of Inflammatory Cells

To assess the inflammatory response during arterialization in this model, we stained vessels for E-selectin and VCAM-1, inducible endothelial-expressed adhesion molecules. The presence of inflammatory cells was also studied using Gr-1, a marker specific for neutrophils, and Mac-1, a marker for monocytes and macrophages. Twenty-four hours after surgery, E-selectin was sporadically expressed in a few endothelial cells (Figure 6B), and there was little expression of VCAM-1 at this time point (Figure 6F). Neutrophils appeared in the vascular wall after 1 day of exposure to the arterial circulation (Figure 6J). Furthermore, some monocytes and macrophages were present along the lumen and vascular wall after 1 day (Figure 6N). At 3 days, there was an increase in E-selectin (Figure 6C) and VCAM-1 (Figure 6G) expression in the endothelium with a concomitant influx of neutrophils and macrophages appearing in all layers of the vascular wall (Figure 6, K and O). It is possible that some of these inflammatory cells were recruited from the circulation in response to the increased expression of E-selectin and VCAM-1 on endothelial cells. Interestingly, after 7 days of arterialization, the inflammatory response appeared resolved with no expression of E-selectin (Figure 6D) or VCAM-1 (Figure 6H), and no evidence of neutrophils or macrophages in the vascular wall (Figure 6, L and P). At all time points studied, control vessels demonstrated little evidence of inflammation with no E-selectin expression (Figure 6A), minimal VCAM-1 expression (Figure 6E), and no neutrophils or macrophages were present in the vascular wall (Figure 6I, 6 mol/L). Non-surgical control vessels in Figure 6 were taken from mice 3 days after surgery, and days 1 and 7 control vessels are not shown. Sham surgery vessels at 1 day and 3 days demonstrated minimal expression of E-selectin and VCAM-1 (data not shown).

Vascular Permeability

To determine whether the arterialized vein exhibits functional changes in comparison to the native jugular vein, we tested for differences in vascular permeability. After intravenous Evans Blue dye injection, the contralateral control JV demonstrated extravasation of Albumin-Evans Blue in the vascular wall, and minimal extravasation was seen in the control CCA. Under these conditions, the aorta remained predominantly unstained, with some

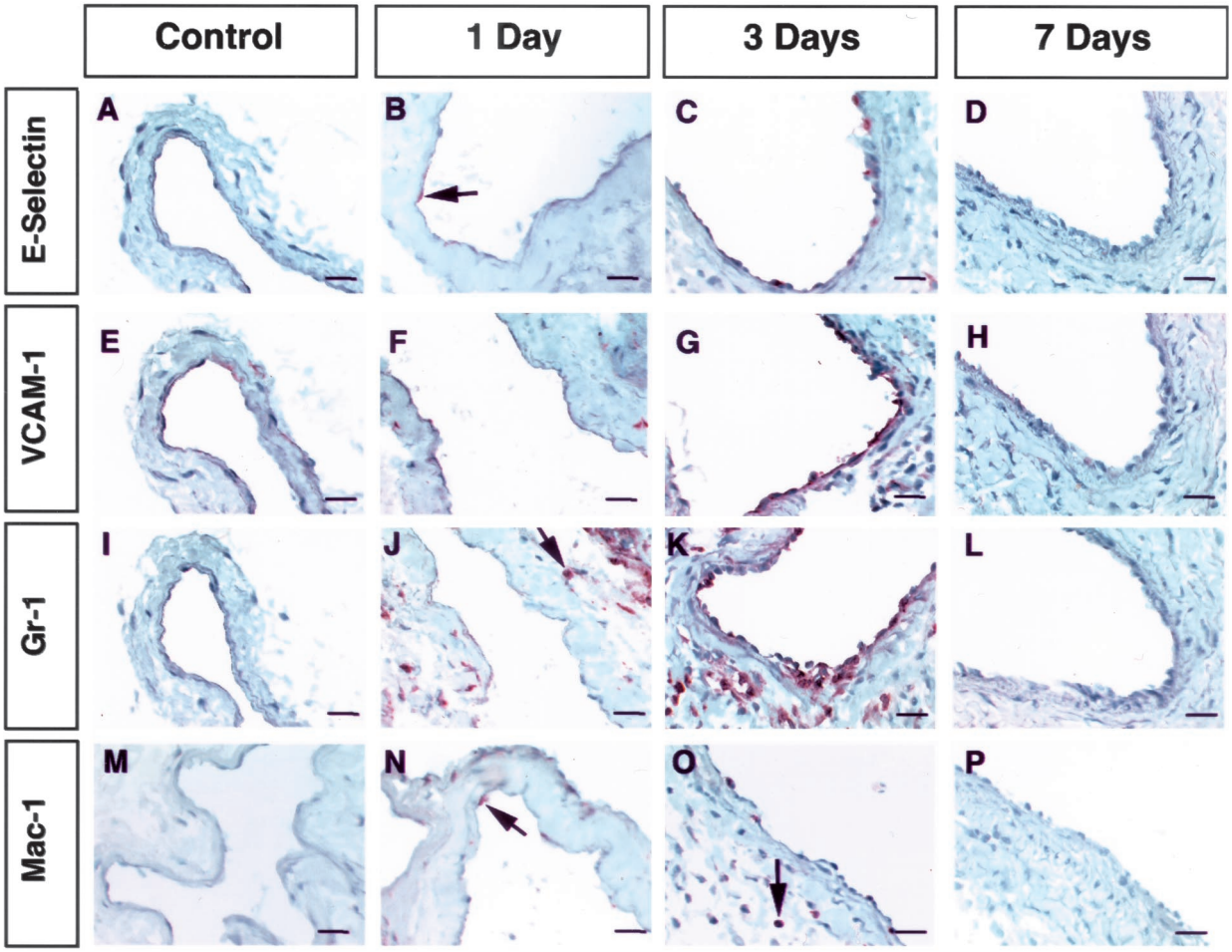

Figure 6. Markers of inflammation and inflammatory cells during venous arterialization. **A:** There is no evidence of E-selectin expression in the contralateral control external jugular vein (JV). **B:** E-selectin is weakly expressed in few endothelial cells 24 hours after surgery (**arrow**). **C:** E-selectin expression increases 3 days after surgery. **D:** After 7 days of arterialization, E-selectin expression is absent. **E:** The control JV demonstrates minimal VCAM-1 expression. **F:** VCAM-1 expression is minimally present 24 hours after surgery. **G:** Three days after surgery, VCAM-1 expression is highly up-regulated in the vessel. **H:** VCAM-1 expression is absent after 7 days of arterialization. **I:** There are no neutrophils in the control JV. **J:** Neutrophils appear in the vascular wall 1 day after surgery. **K:** Neutrophils are present in the vascular wall and lumen 3 days after surgery. **L:** At 7 days, the neutrophils are absent from the vascular wall and lumen. **M:** The control JV does not show the presence of monocytes or macrophages. **N:** There are a few monocytes and macrophages in the vascular wall 1 day after surgery. **O:** Monocytes and macrophages are present in the vascular wall 3 days after surgery. **P:** At 7 days, there are no macrophages or monocytes. **Bars**, 30 μm.

Evans Blue dye extravasation at the aortic arch (data not shown). The arterialized vein, 7 days after surgery, showed extravasation of dye at the region of the microvascular catheter anastomosis, but remained impermeable 4 mm distally (Figure 7A). Similar results were obtained using vessels that had been exposed to the arterial circulation for 1 and 3 days (data not shown). Nevertheless, addition of rhVEGF 10 minutes after Evans Blue dye injection resulted in extravasation of dye in the arterialized vein with a concomitant increase in the control CCA, 7 days after surgery (Figure 7B).

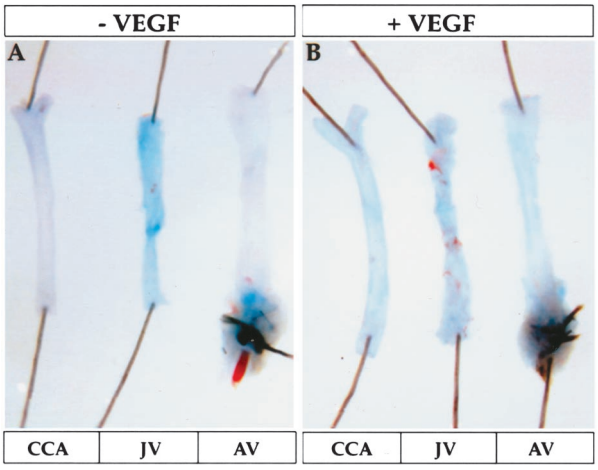

Figure 7. Decrease of endothelium-dependent vascular permeability in the arterialized vein. **A:** Seven days after surgery, the arterialized vein (AV) does not extravasate Albumin-Evans Blue dye distal to the microvascular catheter anastomosis. The contralateral external jugular vein (JV) extravasates Evans Blue, however the common carotid artery (CCA) demonstrates minimal extravasation. **B:** After intravenous rhVEGF injection, all vessels extravasate Evans Blue dye. The red **spots** seen on tissues are coagulated blood.

Discussion

This report presents a new model of venous arterialization in mice, in this model, the external jugular vein was exposed to the carotid arterial circulation *in situ* (arteriovenous connection), thus the arterialized venous segment was never exteriorized from the body of the animal. Although this model does not recapitulate pathophysio-

logical conditions in humans, it displays several early features of venous arterialization previously described in other species. Previously developed mouse models were designed to generate neointimal hyperplastic and atherosclerotic lesions[22,23] by dissection, removal, and storage of vessels before their interposition into the arterial circulation. These significant variations of the surgical procedure may explain the differences in the remodeling process observed 7 days after surgery. For example, we demonstrated proliferation of smooth muscle cells, the formation of smooth muscle cell layers, and minimal apoptosis in the vascular wall 7 days post-surgery. However, Zou et al [22] showed significant cell loss and vessel degeneration at 7 days. In our model, we showed that the vascular endothelium is preserved at all time points studied. Prior studies have demonstrated that the endothelium is vulnerable to disruption following surgical manipulation, and that its presence is necessary for vascular remodeling. In a well-established model of flow reduction, alterations of vessel geometry in response to changes in blood flow were shown to be endothelium dependent[27] and primarily mediated by endothelial-derived nitric oxide.[28] Thus, our observations suggest that the presence of an intact endothelium influences the morphological features seen in the early adaptations of a venous segment interposed into the arterial circulation. Our findings are consistent with long-term studies in humans showing that smooth muscle cells migrate into the vascular intima, proliferate, and produce extracellular matrix in saphenous vein grafts.[29] However, the precise origin of the smooth muscle cells in this model remains unknown.

Previous studies suggest that positive remodeling of an arteriole to an artery is influenced by modulators of inflammation. For example, in a rabbit model of collateral circulation arteriogenesis, the expression of ICAM-1 and VCAM-1 preceded the appearance of monocytes.[30] Furthermore, leukocyte adherence has been reported in areas of endothelial injury in canine bypass grafts.[8] We also observed the expression of adhesion molecules and inflammatory cells in this model at 1 and 3 days after surgery. Interestingly, Zou et al[31] showed in their mouse model of neointima formation in venous bypass grafts that the absence of intercellular adhesion molecule-1 expression resulted in diminished intimal lesion formation, reduced leukocyte adhesion, and lower monocyte/macrophage accumulation in neointimal lesions. This fundamental connection between inflammatory mediators and vascular remodeling underscores the influence of cellular interactions in affecting phenotypic modulations. Thus, the temporal coordination of VCAM-1 and E-selectin expression together with the presence of neutrophils, monocytes/macrophages in this model may contribute to the structural changes observed.

To begin to characterize the functional adaptation of the arterialized vessel in this model, we examined whether the arterialization process could modulate vascular permeability. Previous studies have shown that venules are more permeable than arterioles and capillaries, demonstrating an arteriovenous gradient of permeability in normal vessels.[32,33] Regional differences in vascular permeability have also been characterized *in vivo*. In rabbits, permeability is enhanced in the aortic arch and aortic ostia,[34] which is consistent with areas of low-density lipoprotein (LDL) retention and hemodynamic variation.[35] To demonstate that the decrease in permeability is endothelium-mediated we intravenously injected mice with VEGF. The addition of VEGF caused an increase in permeability with extravasation of Albumin-Evans Blue Dye in all vessels. In rats, VEGF was shown to increase capillary and venular permeability by opening endothelial intercellular junctions and inducing fenestrae in the endothelium.[36] In this model, the decrease in permeability of the arterialized vein in comparison to the normal external jugular vein reflects functional changes in the endothelial phenotype and/or alterations of the normal endothelial-intimal architecture.

In summary, we have developed a novel mouse model of venous arterialization that defines early cellular and molecular adaptations of a venous vessel in response to a new local arterial biomechanical environment. The use of this model in the context of the genetic and genomic tools available in mice should help in the identification and functional characterization of genes implicated in venous arterialization.

Acknowledgments

We thank Dr. Ronit Satchi-Fainaro for guidance with the vascular permeability assay; Dr. Lynn Chang, Dr. Mark Puder, and Parker Wilson for help at early stages of the surgical procedure; and Jeanne-Marie Kiely for helpful comments on the manuscript.

References

1. Garrett HE, Diethrich EB, Debakey ME: Myocardial revascularization. Surg Clin North Am 1996, 46:863–871
2. Gibbons GH, Dzau VJ: The emerging concept of vascular remodeling. N Engl J Med 1994, 330:1431–1438
3. Charles AK, Gresham GA: Histopathological changes in venous grafts and in varicose and non-varicose veins. J Clin Pathol 1993, 46:603–606
4. McCabe M, Cunningham GJ, Wyatt AP, Rothnie NG, Taylor GW: A histological and histochemical examination of autogenous vein grafts. Br J Surg 1967, 54:147–154
5. Mavromatis K, Fukai T, Tate M, Chesler N, Ku DN, Galis ZS: Early effects of arterial hemodynamic conditions on human saphenous veins perfused ex vivo. Arterioscler Thromb Vasc Biol 2000, 20:1889–1895
6. Galis ZS, Hkatri JJ: Matrix metalloproteinases in vascular remodeling and atherogenesis: the good, the bad, and the ugly. Circ Res 2002, 90:251–262
7. Wallner K, Li C, Fishbein MC, Shah PK, Sharifi BG: Arterialization of human vein grafts is associated with tenascin-C expression. J Am Coll Cardiol 1999, 34:871–875
8. Bush HJ, Jakubowski JA, Curl GR, Deykin D, Nabseth DC: The natural history of endothelial structure and function in arterialized vein grafts. J Vasc Surg 1986, 3:204–215
9. Fann JI, Sokoloff MH, Sarris GE, Yun KL, Kosek JC, Miller DC: The reversibility of canine vein-graft arterialization. Circulation 1990, 92: IV-9-IV-18
10. Henderson VJ, Mitchell RS, Kosek JC, Cohen RG, Miller DC: Biochemical (functional) adaptation of "arterialized" vein grafts. Ann Surg 1986, 203:339–345

11. Saenz NC, Hendren RB, Schoof DD, Folkman J: Reduction of smooth muscle hyperplasia in vein grafts in athymic rats. Lab Invest 1991, 65:55–22
12. Davies MG, Hagen PO: Bradykinin receptor modulation in vein grafts. J Invest Surg 1994, 7:493–501
13. Davies MG, Klyachkin ML, Svendsen E, Hagen PO: A comparative study of endothelium-derived relaxing factor-mediated relaxation and smooth muscle cell function in arterial and venous vein bypass grafts. Cardiovasc Surg 1996, 4:150–160
14. Davies MG, Ramkumar V, Hagen PO: Adenosine responses in experimental vein bypass grafts. J Vasc Surg 1998, 28:929–938
15. Davies MG, Huynh TT, Hagen PO: Characterization of dopamine-mediated relaxation in experimental vein bypass grafts. J Surg Res 2000, 92:103–107
16. Channon KM, Fulton GJ, Davies MG, Peters KG, Ezekowitz MD, Hagen PO, Annex BH: Modulation of tissue factor protein expression in experimental venous bypass grafts. Arterioscler Thromb Vasc Biol 1997, 17:1313–1319
17. Fulton GJ, Channon KM, Davies MG, Annex BH, Hagen PO: Alterations in collagen subtype III and IV protein in experimental venous bypass grafting. Coron Artery Dis 1998, 9:191–197
18. Eguchi D, Nishimura J, Kobayashi S, Komori K, Sugimachi K, Kanaide H: Down-regulation of endothelin B receptors in autogenous saphenous veins grafted into the arterial circulation. Cardiovasc Res 1997, 35:360–367
19. Kim AY, Walinsky PL, Kolodgie FD, Bian C, Sperry JL, Deming CB, Peck JG, Ang GB, Sohn RS, Esmon CT, Virmani R, Stuart RS, Rade JJ: Early loss of thrombomodulin expression impairs vein graft thromboresistance: implications for vein graft failure. Circ Res 2002, 90:205–212
20. Hamdan AD, Aiello LP, Misare BD, Contreras MA, King GL, Logerfo FW, Quist WC: Vascular endothelial growth factor expression in canine peripheral vein bypass grafts. J Vasc Surg 1997, 26:79–86
21. Westerband A, Crouse D, Richter LC, Aguirre ML, Wixon CC, James DC, Mills JL, Hunter GC, Heimark RL: Vein adaptation to arterialization in an experimental model. J Vasc Surg 2001, 33:561–569
22. Zou Y, Dietrich H, Hu Y, Metzler B, Wick G, Xu Q: Mouse model of venous bypass graft arteriosclerosis. Am J Pathol 1998, 153:1301–1310
23. Zhang L, Hagen PO, Kisslo J, Peppel K, Freedman NJ: Neointimal hyperplasia rapidly reaches steady state in a novel murine vein graft model. J Vasc Surg 2002, 36:824–832
24. Mayr U, Mayr M, Li C, Wernig F, Dietrich H, Hu Y, Xu Q: Loss of p53 accelerates neointimal lesions of vein bypass grafts in mice. Circ Res 2002, 90:197–204
25. Hu Y, Davidson F, Ludewig B, Erdel M, Mayr M, Url M, Dietrich H, Xu Q: Smooth muscle cells in transplant atherosclerotic lesions are originated from recipients, but not bone marrow progenitor cells. Circulation 2002, 106:1834–1839
26. Dietrich H, Hu Y, Zou Y, Huemer U, Metzler B, Li C, Mayr M, Xu Q: Rapid development of vein graft atheroma in ApoE-deficient mice. Am J Pathol 2000, 157:659–669
27. Langille BL, O'Donnell F: Reductions in arterial diameter produced by chronic decreases in blood flow are endothelium-dependent. Science 1986, 231:405–407
28. Rudic RD, Shesely EG, Maeda N, Smithies O, Segal SS, Sessa WC: Direct evidence for the importance of endothelium-derived nitric oxide in vascular remodeling. J Clin Invest 1998, 101:731–736
29. Newby AC, George SJ: Proliferation, migration, matrix turnover, and death of smooth muscle cells in native coronary and vein graft atherosclerosis. Curr Opin Cardiol 1996, 11:574–582
30. Scholz D, Ito W, Fleming I, Deindl E, Sauer A, Wiesnet M, Busse R, Schaper J, Schaper W: Ultrastucture and molecular histology of rabbit hind-limb collateral artery growth (arteriogenesis). Virchows Arch 2000, 436:257–270
31. Zou Y, Hu Y, Mayr M, Dietrich H, Wick G, Xu Q: Reduced neointima hyperplasia of vein bypass grafts in intercellular adhesion molecule-1-deficient mice. Circ Res 2000, 86:434–440
32. Rous P, Gilding HP, Smith F: The gradient of vascular permeability. J Exp Med 1930, 51:807–830
33. Bundit V, Wissig SL: Surgical exposure induces formation of an arteriovenous permeability gradient for macromolecules in the microcirculation of muscle. Microvasc Res 1986, 31:235–249
34. Barakat AI, Uhthoff PA, Colton CK: Topographical mapping of sites of enhanced HRP permeability in the normal rabbit aorta. J Biomech Eng 1992, 114:283–292
35. Nielsen LB, Nordestgaard BG, Stender S, Kjeldsen K: Aortic permeability to LDL as a predictor of aortic cholesterol accumulation in cholesterol-fed rabbits. Arterioscler Thromb 1992, 12:1402–1409
36. Roberts WG, Palade GE: Increased microvascular permeability and endothelial fenestration induced by vascular endothelial growth factor. J Cell Sci 1995, 108:2369–2379